Philosophical Transactions of the Royal Society London A **360** (2002) 303-315.

Chaos and fractals in dynamical models of transport and reaction

P. Gaspard and I. Claus
Center for Nonlinear Phenomena and Complex Systems,
Faculté des Sciences, Université Libre de Bruxelles,
Campus Plaine, Code Postal 231, B-1050 Brussels, Belgium

This paper contains a discussion of dynamical randomness among the different methods of simulation of a fluid and its characterization by the concept of Kolmogorov-Sinai entropy per unit time. Moreover, a renormalization-group method is presented in order to construct the hydrodynamic and reactive modes of relaxation in chaotic models. The renormalization-group construction allows us to obtain the dispersion relation of these modes, i.e., their damping rate versus the wavenumber. Besides, these modes are characterized by a fractal dimension given in terms of a diffusion coefficient and a Lyapunov exponent.

I. INTRODUCTION

Recent work has shown the importance of dynamical chaos in the context of the simulation of the motion of particles composing fluids. Dynamical chaos is characterized by positive Lyapunov exponents which are the rate of exponential separation between nearby trajectories. Many simulations have shown that typical systems of interacting particles such as fluids of hard spheres or Lennard-Jones particles have positive Lyapunov exponents [1–3].

The purpose of the present paper is to investigate the consequences of this deterministic chaos, especially, in our understanding of the properties of fluctuations and of relaxation toward the thermodynamic equilibrium either by transport or reaction processes.

In Section II, we show that the dynamical randomness of the stochastic fluctuations in the motion of particles in a fluid can be characterized by the so-called Kolmogorov-Sinai (KS) entropy per unit time, which provides a way to compare deterministic and random models. This result suggests an understanding of the dynamical randomness of the stochastic fluctuations as a manifestation of the sensitivity to initial conditions in the underlying deterministic dynamics, as far as the bulk behaviour of the fluid is concerned.

Thereafter, in Section III, we investigate some consequences of chaos in simple deterministic models of diffusion and we show that unexpected fractals appear in this context.

In Section IV, these results are extended to reaction-diffusion systems, leading to the construction of the reactive modes of relaxation and to the investigation of their properties in the rate-limited and diffusion-limited regimes.

Conclusions are drawn in Section V.

II. DYNAMICAL RANDOMNESS AND CHAOS

The simulation of fluids can be carried out by a large variety of different methods starting from the integration of Navier-Stokes equations, down to the integration of Newton's equations ruling the motion of particles composing the fluid. The microscopic degrees of freedom of the fluid do not show up at the macroscopic level. Therefore, in the Navier-Stokes equations, the microscopic dynamics is hidden in the value of a few coefficients such as viscosity, heat conductivity, or reaction rates. For this reason, it is not always required to simulate the microscopic dynamics and intermediate descriptions have been proposed in terms of lattice gas automata and the lattice Boltzmann method [4–11], in which the microscopic description is replaced by a simplified mesoscopic description which is numerically efficient. Today, there exists a large variety of different methods and it becomes important to compare their properties.

In this regard, we notice that an important distinction exists between the methods which simulate the individual trajectories of some particles and the other ones in which average observable quantities are evolved in time. In the former class, we find the molecular dynamics method (integration of Newton's equations), the kinetic Monte-Carlo methods such as Bird's method, the lattice gas automata, the Langevin processes, the birth-and-death processes for chemical reactions such as Gillespie's method, etc... In the latter class, we find the Boltzmann equation and other nonlinear kinetic equations, the lattice Boltzmann method, the macroscopic equations such as Navier-Stokes equations, and others. In the latter class, we also find the master equations of the processes of the former class such as the Liouville equation, the Fokker-Planck equation, and other Chapman-Kolmogorov master equations. We notice that these master equations are necessarily linear as required by probability theory. The central difference

between both classes of methods comes from the microscopic dynamical randomness in the former class although this dynamical randomness is no longer the feature of the latter class because of averaging.

The dynamical randomness is evident in all the methods of the former class except for the molecular dynamics methods, which seems to contradict the above classification. However, it has been noticed for long [12] that the simulation of the Newtonian motion of particles in a fluid is highly unstable and that a perturbation $\delta\mathbf{X}_0$ on the initial conditions $\mathbf{X}_0$ grows exponentially in the early time steps as

$$\|\delta\mathbf{X}_t\| \simeq \|\delta\mathbf{X}_0\| \ \exp(\lambda_i t) \tag{1}$$

which defines a positive Lyapunov exponent λ_i associated with some unstable direction of the microscopic motion in phase space. This sensitivity to initial conditions generates dynamical randomness over long times in a phenomenon known today as deterministic chaos [13]. The remarkable result is that deterministic chaos resolves the aforementioned contradiction. Thanks to the discovery of deterministic chaos, it becomes clear that dynamical randomness is the feature of all the methods of the former class.

Recent work has shown that this result can be confirmed by a mathematical quantity called the KS entropy per unit time, which measures the amount of randomness developed during one time unit of the evolution [14]. For deterministic chaos in a bounded phase space, the KS entropy is equal to the sum of the positive Lyapunov exponents

$$h_{\mathrm{KS}} = \sum_{\lambda_i > 0} \lambda_i \tag{2}$$

which is known as Pesin's theorem [13].

For Markov chains defined by the probabilities $P_{\omega\omega'}$ of transition between the states ω and ω' the KS entropy is given by [15]

$$h_{\mathrm{KS}} = -\sum_{\omega\omega'} p_\omega \ P_{\omega\omega'} \ \ln P_{\omega\omega'} \tag{3}$$

where p_ω is the stationary probability of the state ω. Lattice gas automata are examples of such Markov chains. In this case, the KS entropy is a measure of the rate of production of information due to the call of a pseudo-random generator by the simulation method. For the simulation of a simple coin flipping process, the random variable takes the values 0 or 1 with probabilities $(\frac{1}{2}, \frac{1}{2})$ and the KS entropy per coin flipping is equal to $h_{\mathrm{KS}} = \ln 2$. In a lattice gas automaton, the KS entropy depends on the configurations ω of the whole system of particles and will be determined by the collision rules.

Since the lattice gas automaton provides a coarse-grained description of the microscopic motion of particles we should expect that its KS entropy (3) is lower than the KS entropy (2) of the detailed underlying dynamics. We may wonder if such a comparison between the KS entropies is legitimate. The fact is that pseudo-random generators are often based on the linear congruence method which generates a sequence $I_0, I_1, I_2, I_3, ...$ of integers by the iteration

$$I_{n+1} = A \ I_n + B \qquad (\mathrm{mod}.C) \tag{4}$$

A, B and C being adequately chosen integers. This iteration is nothing else than a discretized version of a well-known chaotic map with a positive Lyapunov exponent equal to $\lambda = \ln A$. On the other hand, in deterministic chaos, such a randomness is self-generated by the dynamics because of the instability characterized by the positive Lyapunov exponents λ_i. Accordingly, the comparison between both types of dynamical randomness is highly relevant.

Consequences of this observation for lattice gas automata and lattice Lorentz gases have been developed elsewhere [16, 17]. Recently, other interesting discrete models called graphs have also been studied [18].

The dynamical randomness of stochastic processes such as the Langevin or the birth-and-death processes can also be characterized by the related concept of (ε, τ)-entropy per unit [19]. These entropies allow us to compare the different processes for their dynamical randomness.

We notice that the simulation methods of the latter class based on some average observable quantities can often be nonlinear. In this case, their dynamics may have positive Lyapunov exponents. A famous example is given by the Navier-Stokes equations in turbulent regimes. This deterministic chaos appears on larger spatial scales than the microscopic chaos of the molecular dynamics. Indeed, turbulence is a macroscopic phenomenon. Consequently, such deterministic chaos are characterized by much smaller Lyapunov exponents or KS entropies than the microscopic chaos and they occur on much longer time scales. In particular, the onset of turbulence is well known as a phenomenon of macroscopic chaos.

Because of the difference of time scales between macroscopic and microscopic chaos, the chaotic motion in the microscopic dynamics of the particles composing a fluid would appear as a diffusive noise on the time scale of the macroscopic motions of the fluid, such as convection and turbulence. In flowing systems, the advection of particles

can therefore present both microscopic and macroscopic randomnesses, which manifest themselves on different spatial scales (if the Reynolds number is not too high) [19].

In the perspective above, typical models of statistical mechanics turn out to have a positive KS entropy per unit time at the particle level of description. If we suppose that a random simulation method is set up by coarse-graining an underlying deterministic dynamics of the fluid, the comparison between the KS entropies (2) and (3) leads us to the conclusion that the underlying deterministic dynamics should be chaotic and characterized by positive Lyapunov exponents. Many simulations going back to pioneering works have nowadays brought rich and detailed evidence that models of statistical mechanics have positive Lyapunov exponents [1–3, 12]. It is therefore of great importance to investigate the consequences of this chaos, which is the purpose of the following section.

III. RELATIONSHIPS BETWEEN CHAOS AND TRANSPORT

A. Chaotic models of diffusion

The transport property of diffusion is already the feature of simple dynamical systems such as the periodic Lorentz gases, in which independent point particles move in a two-dimensional lattice of scatterers. The Hamiltonian of such systems is given by

$$H = \frac{p_x^2 + p_y^2}{2m} + \sum_{\mathbf{l}\in\mathcal{L}} V(\|\mathbf{r} - \mathbf{l}\|) \tag{5}$$

where $\mathbf{l}$ is a vector of a periodic lattice $\mathcal{L}$. The potential can be an attractive Yukawa potential $V(r) = -\exp(-\alpha r)/r$ or a hard-core potential. In the latter case, each point particle undergoes elastic collisions on hard disks fixed in the plane.

For the case of a square lattice of Yukawa potentials, the dynamics has been proved to be chaotic and diffusive at high enough energy [20]. For the case of a triangular lattice of hard disks, the dynamics is known to be chaotic and diffusive if the horizon is finite, i.e., if the density of hard disks is high enough [21].

In the Lorentz gases, the dynamics evolves continuously with time (see Figs. 1b and 1c). This continuous-time dynamics can be replaced by a discrete-time dynamics by considering a Poincaré surface of section in the phase space of the flow. In the case of the hard-disk Lorentz gas, a natural Poincaré surface of section is defined by the border of the disks where the elastic collisions occur. In this way, it is possible to reduce the dynamics to a mapping which rules the successive collisions of the particle with the disks [14]. The Poincaré surface of section can be represented as a lattice of squares. Each square is associated with a disk. The horizontal coordinate of each square is the angle of the point of impact at which the particle collides with the disk, while the vertical coordinate is the component of the velocity which is parallel to the border of the disk. The mapping is known to be area-preserving in this representation [14]. The mapping acts by stretching each square, cutting it in several pieces, and redistributing the pieces onto the different disks of the lattice. This mapping is nonlinear and non-trivial, but its main features can be captured by piecewise-linear mappings of baker type (see Fig. 1a), following the pioneering work of Seidel [22] and Hopf [23].

This line of reasoning has motivated the introduction of the multibaker models of diffusion, which are fully chaotic and exactly solvable [24]. The study of multibaker models has led to the discovery of relationships between chaos and diffusion, which have turned out to be general and to extend *mutatis mutandis* to such flows as the Lorentz gases. The connection between the Lorentz gases and the multibaker models is nowadays very well documented [14, 25]. The following subsection presents a recently discovered relationship between chaos and diffusion.

B. Fractality of the hydrodynamic modes of diffusion

At the macroscopic level, diffusion is described by the following equation for the density $n(\mathbf{r}, t)$ of tracer particles:

$$\partial_t\, n = \mathcal{D}\, \nabla^2 n \tag{6}$$

where $\mathcal{D}$ is the diffusion coefficient. This equation admits special solutions which are spatially periodic with a wavelength ℓ and a corresponding wavenumber $k = 2\pi/\ell$, and which are exponentially damped in time:

$$n(\mathbf{r}, t) \sim \exp(i\mathbf{k}\cdot\mathbf{r})\ \exp(-\mathcal{D}\, k^2\, t) \tag{7}$$

The longer the wavelength, the slower the damping because of the conservation of mass. These special solutions are called the hydrodynamic modes of diffusion. Such hydrodynamic modes exist associated with the different transport

properties such as viscosity, heat conductivity, etc. Such hydrodynamic modes have been studied experimentally, especially, by Professor Jean Pierre Boon thanks to light scattering techniques [26].

In nonequilibrium statistical mechanics, a central question is to know if such hydrodynamic modes exist at the microscopic phase-space level of description of the fluid. Recent work on chaotic models of diffusion has shown that the answer is affirmative and that the hydrodynamic modes of diffusion are given by singular distributions (without density function) which are mapped onto themselves up to a renormalizing factor which is exponentially damped in time [27]. The singular character of the distributions explains the well-known statement that coarse-graining is required for nonequilibrium statistical mechanics because a singular distribution acquires a meaning as a number only when integrated with a test function such as the indicator function of a cell in phase space. The recent work goes however beyond this statement in showing that the hydrodynamic modes are defined for arbitrarily fine coarse-graining and, thus, independently of a particular coarse-graining. In particular, we can define a cumulative function associated with each singular distribution by continuously varying the size of the phase-space set over which the distribution is cumulated. It turns out that these cumulative functions form fractal curves in the complex plane having a dimension which is independent of the phase-space set chosen to define the cumulative function. The cumulative function of a diffusive hydrodynamic mode of wavenumber $\mathbf{k}$ can be constructed by

$$F_{\mathbf{k}}(\xi) = \lim_{t\to\infty} \frac{\int_a^{\xi} d\xi' \exp\left[i\mathbf{k}\cdot(\mathbf{r}_t - \mathbf{r}_0)_{\xi'}\right]}{\int_a^{b} d\xi' \exp\left[i\mathbf{k}\cdot(\mathbf{r}_t - \mathbf{r}_0)_{\xi'}\right]} \tag{8}$$

$\mathbf{r}_t$ denotes the position at current time t of the particle moving in the system under Newton's equations and starting from the initial condition $\mathbf{r}_0(\xi')$. The cumulative function (8) is obtained by averaging over all the initial conditions taken along a line in phase space which is parametrized by the variable $\xi \in [a, b]$. This line must be transverse to the unstable directions in phase space because the distribution representing the hydrodynamic mode is singular in the stable directions but smooth in the unstable directions. In the multibaker map, we can take ξ as the vertical coordinate y since the vertical axis coincides with the stable direction: $\xi = y \in [0, 1]$. In the Lorentz gases, the stable directions are non-trivial and we can take the line as a circle around a scatterer with the velocity normal to the circle. The parameter is thus an angle on the circle: $\xi = \theta \in [0, 2\pi]$.

In Eq. (8), the numerator defines a curve parametrized by ξ in the complex plane at fixed time t. This numerator is given by averaging the phase $\exp(i\mathbf{k}\cdot\Delta\mathbf{r}_t)$ over all the initial conditions in the interval $\xi' \in [0, \xi]$. Since a famous work by Van Hove [28], such averages $\langle\cdot\rangle$ are known to decay exponentially at long times and to define the dispersion relation of diffusion:

$$s_{\mathbf{k}} = \lim_{t\to\infty} \frac{1}{t} \ln \langle \exp\left[i\mathbf{k}\cdot(\mathbf{r}_t - \mathbf{r}_0)\right]\rangle = -\,\mathcal{D}\,k^2 + \mathcal{O}(k^4) \tag{9}$$

In Eq. (8), the role of the denominator is to renormalize the numerator by a ξ-independent quantity which also decays exponentially according to (9). Therefore, we can define, in the complex plane, a curve which admits a limit at long times. The so-defined function $F_{\mathbf{k}}(\xi)$ is then the cumulative function of a state which is exponentially damped under the exact dynamics with a rate given by the dispersion relation (9). This state is precisely what should be identified with the hydrodynamic mode of diffusion.

Fig. 2 depicts the cumulative functions of the hydrodynamic modes for the area-preserving dyadic multibaker mapping as well as for the two aforementioned Lorentz gases. The curves are fractals in the complex plane and their Hausdorff dimension increases with the wavenumber k according to

$$D_{\mathrm{H}} = 1 + \frac{\mathcal{D}}{\lambda}\,k^2 + \mathcal{O}(k^4) \tag{10}$$

where λ is the positive Lyapunov exponent of the system and $\mathcal{D}$ its diffusion coefficient [27, 29].

The relationship between the properties of chaos and diffusion established by Eq. (10) is very similar to another formula previously obtained in the escape-rate theory [30, 31]:

$$d_{\mathrm{H}} = 1 - \frac{\mathcal{D}}{\lambda}\,\left(\frac{\pi}{L}\right)^2 + \mathcal{O}\left(\frac{1}{L^3}\right) \tag{11}$$

Here d_{H} is the partial Hausdorff dimension of a fractal repeller composed of the trajectories which are forever trapped in a region delimited by two absorbing walls separated by the distance L. The same positive Lyapunov exponent λ appears in both Eqs. (10) and (11). In the case of the fractal repeller, the decaying mode has a wavelength equal to twice the distance L: $\ell = 2L$. The wavenumber is therefore $k = 2\pi/\ell = \pi/L$ so that both Eqs. (10) and (11) are identical in this respect. There remains a difference between the Hausdorff dimensions themselves since they characterize different types of objects in different spaces: $1 \leq D_{\mathrm{H}} \leq 2$ characterizes a curve in the complex plane while $0 \leq d_{\mathrm{H}} \leq 1$ is the partial dimension in the stable or unstable directions of a fractal repeller defined in the phase space.

C. Nonequilibrium steady states of diffusion

The nonequilibrium steady states corresponding to a linear profile of concentration between two reservoirs separated by a large distance can be obtained directly from the hydrodynamic modes by the following reasoning [14, 32].

It is well-known that the macroscopic diffusion equation (6) admits stationary solutions which are linear in position in the direction of the gradient $\mathbf{g}$ of concentration: $n \sim \mathbf{g} \cdot \mathbf{r}$. Such steady states can be obtained from hydrodynamic modes of the form $n \sim \sin(\mathbf{k} \cdot \mathbf{r}) = [\exp(+i\mathbf{k} \cdot \mathbf{r}) - \exp(-i\mathbf{k} \cdot \mathbf{r})]/(2i)$. Indeed, in the limit of arbitrary small wavenumbers $\mathbf{k} = \mathbf{g} \to 0$, the sine profile of concentration converges to the linear profile $n \sim \mathbf{g} \cdot \mathbf{r}$ between two reservoirs located at fixed positions $\mathbf{g} \cdot \mathbf{r} = \pm \|\mathbf{g}\| L/2$.

A similar reasoning can be applied to the microscopically defined hydrodynamic mode by expanding their cumulative function (8) in powers of the wavenumber $\mathbf{k} = \mathbf{g}$ while keeping the linear term. This procedure defines the cumulative function of the nonequilibrium steady state corresponding to a gradient $\mathbf{g}$ of concentration as

$$T_{\mathbf{g}}(\xi) = -\, i\, \mathbf{g} \cdot \frac{\partial}{\partial \mathbf{k}} F_{\mathbf{k}}(\xi) \bigg|_{\mathbf{k}=0} \tag{12}$$

Fig. 3 depicts the cumulative functions of the nonequilibrium steady states corresponding to the hydrodynamic modes of Fig. 2. We observe that these cumulative functions have a self-similar structure reminiscent of the fractal curves of Fig. 2. However, the cumulative functions of the steady states have a Hausdorff dimension equal to unity. In the case of the dyadic multibaker map, the cumulative function is known as the Takagi function which is continuous but non-differentiable [32]. The two other cumulative functions in Figs. 3b and 3c are therefore generalizations of the Takagi function for the Lorentz gases.

IV. REACTION-DIFFUSION IN CHAOTIC DYNAMICAL SYSTEMS

We consider simple models of reaction-diffusion in which a point particle diffuses under the deterministic dynamics of a Lorentz gas or a multibaker map and has furthermore a color A or B which changes with probability p_0 every time the particle has a passage through some surfaces inside the phase space. The change of color constitutes a model for a reaction of isomerization $A \leftrightarrow B$. In the case of the hard-disk Lorentz gas, the particle is supposed to change its color upon collision on some of the hard disks, which are referred to as the catalysts. One over N disks is supposed to be a catalyst [33, 34].

If f_A and f_B are the phase-space probability densities to find the particle with colors A and B we notice that the total density $f_A + f_B$ evolves in time precisely under the same deterministic dynamics as the purely diffusive Lorentz gases or multibaker maps. Accordingly, the time evolution of the total density is ruled by the hydrodynamic modes of diffusion already described in the previous section.

However, the difference $f_A - f_B$ of densities has a time evolution of its own which depends, in particular, on the probability p_0 of reaction. This probability introduces an element of randomness in the time evolution of the color. Nevertheless, this randomness manifests itself only in the aforementioned surfaces which are of lower dimension than the phase space itself. This randomness does not prevent the generation of fractal modes of relaxation in the evolution of the color, as evidenced by Fig. 4 which depicts the cumulative functions of the reactive modes of the reactive hard-disk Lorentz gas. The dispersion relation of the reactive modes is given by [33]

$$s_{\mathbf{k}} = -\, 2\, \kappa \; - \; \mathcal{D}^{(\mathrm{r})}\, k^2 + \mathcal{O}(k^4) \tag{13}$$

instead of (9). The Hausdorff dimension of the fractal curves depicted in Fig. 4 is now given by

$$D_{\mathrm{H}} = 1 + \frac{\mathcal{D}^{(\mathrm{r})}}{\lambda^{(\mathrm{r})}}\, k^2 + \mathcal{O}(k^4) \tag{14}$$

where $\mathcal{D}^{(\mathrm{r})}$ is the reactive diffusion coefficient and $\lambda^{(\mathrm{r})}$ an exponent which characterizes the dynamical instability taking also into account the effect of the reaction [34].

The existence of the chemical modes shows that, at the macroscopic level, the densities of the colors evolve in time according to the following reaction-diffusion equations for the color densities n_A and n_B [33]:

$$\partial_t\, n_A \;=\; \mathcal{D}_{AA} \nabla^2 n_A + \mathcal{D}_{AB} \nabla^2 n_B - \kappa (n_A - n_B) \tag{15}$$

$$\partial_t\, n_B \;=\; \mathcal{D}_{BA} \nabla^2 n_A + \mathcal{D}_{BB} \nabla^2 n_B + \kappa (n_A - n_B) \tag{16}$$

where

$$\mathcal{D}_{AA} = \mathcal{D}_{BB} = \frac{\mathcal{D} + \mathcal{D}^{(\mathrm{r})}}{2} \tag{17}$$

are the main diffusion coefficients while

$$\mathcal{D}_{AB} = \mathcal{D}_{BA} = \frac{\mathcal{D} - \mathcal{D}^{(\mathrm{r})}}{2} \tag{18}$$

are cross-diffusion coefficients which are induced by the reaction.

Two regimes can be distinguished:

(1) The *rate-limited* regime where the reaction probability p_0 is low enough with respect to the concentration $1/N$ of catalysts (the limit $p_0 \to 0$). In this regime, the reaction rate is given by [34]

$$\kappa = a\,\frac{p_0}{N} + \mathcal{O}(p_0^2) \tag{19}$$

and the reactive diffusion coefficient by

$$\mathcal{D}^{(\mathrm{r})} = \mathcal{D} + b\,\frac{p_0}{N} + \mathcal{O}(p_0^2) \tag{20}$$

where a and b are model-dependent constants.

(2) The *diffusion-limited* regime where the catalysts are sufficiently diluted for given reaction probability p_0 (the limit $N \to \infty$). In this regime, the reaction rate is given by Smoluchowski's theory and is known to depend on the dimension of the space up to the critical dimension $D = 2$ [33, 35]. This dimension is $D = 1$ for the multibaker and $D = 2$ for the Lorentz gas, in which cases [33, 34]

$$\kappa \simeq \begin{cases} \frac{\mathcal{D}}{2}\left(\frac{\pi}{dN}\right)^2 & \text{for} \quad D = 1 \\ (7.9 \pm 0.3)\,\frac{\mathcal{D}}{d^2 N \ln N} & \text{for} \quad D = 2 \end{cases} \tag{21}$$

where d is the distance between the centers of the squares in the multibaker map or the hard disks in the Lorentz gas. Moreover, the reactive diffusion coefficient decreases below the diffusion coefficient $\mathcal{D}$ as $N \to \infty$ [34].

The result (19) implies that the cross-diffusion coefficient (18) vanish in the limit $p_0 \to 0$ of small reaction probability, which leads to the conclusion that the cross-diffusion effect is induced by the chemical reaction [34]. This cross-diffusion effect is most often neglected in the modeling of reaction-diffusion systems, although the analysis of the chaotic models of reaction-diffusion shows that a non-vanishing cross diffusion can indeed be induced by a reaction. A similar cross-diffusion effect can be expected for a process of spin flip induced by collision in a gas of spin-polarized atoms.

V. CONCLUSIONS

In this paper, we have presented several consequences of chaos in nonequilibrium statistical mechanics.

In Section II, we have shown how chaos is related to the dynamical randomness appearing in the stochastic fluctuations in the motion of particles in fluids. We have shown that this dynamical randomness is the feature, not only of explicitly random methods of simulation, but also of the method of molecular dynamics, which is deterministic. The concept of KS entropy per unit time allows us to compute the dynamical randomness for each method of simulation.

In Section III, we have shown that the exact hydrodynamic modes of diffusion can be constructed in simple chaotic models such as the continuous-time Lorentz gases or the discrete-time multibaker map. At the microscopic phase-space level of description, these hydrodynamic modes turn out to be singular distributions with phase-space scaling properties. Their construction is based on a renormalization using the group of time evolution in phase space. The scaling properties of the hydrodynamic modes are characterized by a fractal dimension, which is related to the diffusion coefficient and to the Lyapunov exponent. Thus, we have here developed a renormalization-group theory for the hydrodynamic modes. Moreover, the nonequilibrium steady states can be directly constructed from the hydrodynamic modes.

These results extend to reaction-diffusion systems, as shown in Section IV where our renormalization-group theory allows us to study in detail the reactive modes of an isomerization reaction $A \leftrightarrow B$ and to obtain their properties in the rate-limited and diffusion-limited regimes. This study shows the existence of a cross-diffusion effect induced by the reaction.

Acknowledgments. This paper is dedicated to Professor Jean Pierre Boon on the occasion of his 65th birthday anniversary. The authors thank Professor G. Nicolis for support and encouragement in this research. The authors are financially supported by the National Fund for Scientific Research (F. N. R. S. Belgium). This research is supported, in part, by the Interuniversity Attraction Pole program of the Belgian Federal Office of Scientific, Technical and Cultural Affairs and by the National Fund for Scientific Research (F. N. R. S. Belgium).

---

[1] R. Livi, A. Politi, and S. Ruffo, *J. Phys. A: Math. Gen.* **19**, 2033 (1986).
[2] H. A. Posch and W. G. Hoover, *Phys. Rev. A* **38**, 473 (1988).
[3] H. van Beijeren, J. R. Dorfman, H. A. Posch, and Ch. Dellago, *Phys. Rev. E* **56**, 5272 (1997).
[4] U. Frisch, D. d'Humières, B. Hasslacher, P. Lallemand, Y. Pomeau, and J.-P. Rivet, Complex Syst. **1**, 649 (1987).
[5] D. H. Rothman and S. Zaleski, Rev. Mod. Phys. **66**, 1417 (1994).
[6] J. P. Boon, D. Dab, R. Kapral, and A. Lawniczak, Phys. Rep. **273**, 55 (1996).
[7] J.-P. Rivet and J. P. Boon, *Lattice Gas Hydrodynamics* (Cambridge University Press, Cambridge UK, 2001).
[8] G. McNamara and G. Zanetti, Phys. Rev. Lett. **61**, 2332 (1988).
[9] R. Benzi, S. Succi, and M. Vergassola, Phys. Rep. **222**, 145 (1992).
[10] S. Chen and G. D. Doolen, Annu. Rev. Fluid Mech. **30**, 329 (1998).
[11] S. Succi, *The Lattice Boltzmann Equation* (Oxford University Press, Oxford UK, 2001).
[12] J. J. Erpenbeck and W. W. Wood, *Molecular Dynamics Techniques for Hard-Core Systems*, in: B. J. Berne, Editor, *Statistical Mechanics, Part B: Time-Dependent Processes* (Plenum Press, New York, 1977) pp. 1-40.
[13] J.-P. Eckmann and D. Ruelle, *Rev. Mod. Phys.* **57**, 617 (1985).
[14] P. Gaspard, *Chaos, Scattering and Statistical Mechanics* (Cambridge University Press, Cambridge UK, 1998).
[15] I. P. Cornfeld, S. V. Fomin, and Ya. G. Sinai, *Ergodic Theory* (Springer-Verlag, Berlin, 1982).
[16] P. Gaspard and J. R. Dorfman, *Phys. Rev. E* **52**, 3525 (1995).
[17] C. Appert, H. van Beijeren, M. H. Ernst, and J. R. Dorfman, Phys. Rev. E **54**, R1013 (1996).
[18] F. Barra and P. Gaspard, Phys. Rev. E **63**, 066215 (2001) (*22 pages*).
[19] P. Gaspard and X.-J. Wang, *Phys. Rep.* **235**, 291 (1993).
[20] A. Knauf, *Commun. Math. Phys.* **110**, 89 (1987); A. Knauf, *Ann. Phys. (N. Y.)* **191**, 205 (1989).
[21] L. A. Bunimovich and Ya. G. Sinai, *Commun. Math. Phys.* **78**, 247, 479 (1980).
[22] W. Seidel, Proc. Natl. Acad. Sci. USA **19**, 453 (1933).
[23] E. Hopf, *Ergodentheorie* (Springer-Verlag, Berlin, 1937).
[24] P. Gaspard, *J. Stat. Phys.* **68**, 673 (1992).
[25] T. Tél and J. Vollmer, *Entropy Balance, Multibaker Maps, and the Dynamics of the Lorentz gas*, in: D. Szász, Editor, *Hard Ball Systems and the Lorentz Gas* (Springer-Verlag, Berlin, 2000) pp. 367-418.
[26] J.-P. Boon and S. Yip, *Molecular Hydrodynamics* (Dover, New York, 1980).
[27] P. Gaspard, I. Claus, T. Gilbert, and J. R. Dorfman, Phys. Rev. Lett. **86**, 1506 (2001).
[28] L. Van Hove, *Phys. Rev.* **95**, 249 (1954).
[29] T. Gilbert, J. R. Dorfman, and P. Gaspard, Nonlinearity **14**, 339 (2001).
[30] P. Gaspard and G. Nicolis, *Phys. Rev. Lett.* **65**, 1693 (1990).
[31] P. Gaspard and F. Baras, *Phys. Rev. E* **51**, 5332 (1995).
[32] S. Tasaki and P. Gaspard, *J. Stat. Phys.* **81**, 935 (1995).
[33] I. Claus and P. Gaspard, J. Stat. Phys. **101**, 161 (2000).
[34] I. Claus and P. Gaspard, *The fractality of the relaxation modes in deterministic reaction-diffusion systems* (preprint ULB, 2001).
[35] I. Claus and P. Gaspard, Phys. Rev. E **63**, 036227 (2001) (*10 pages*).

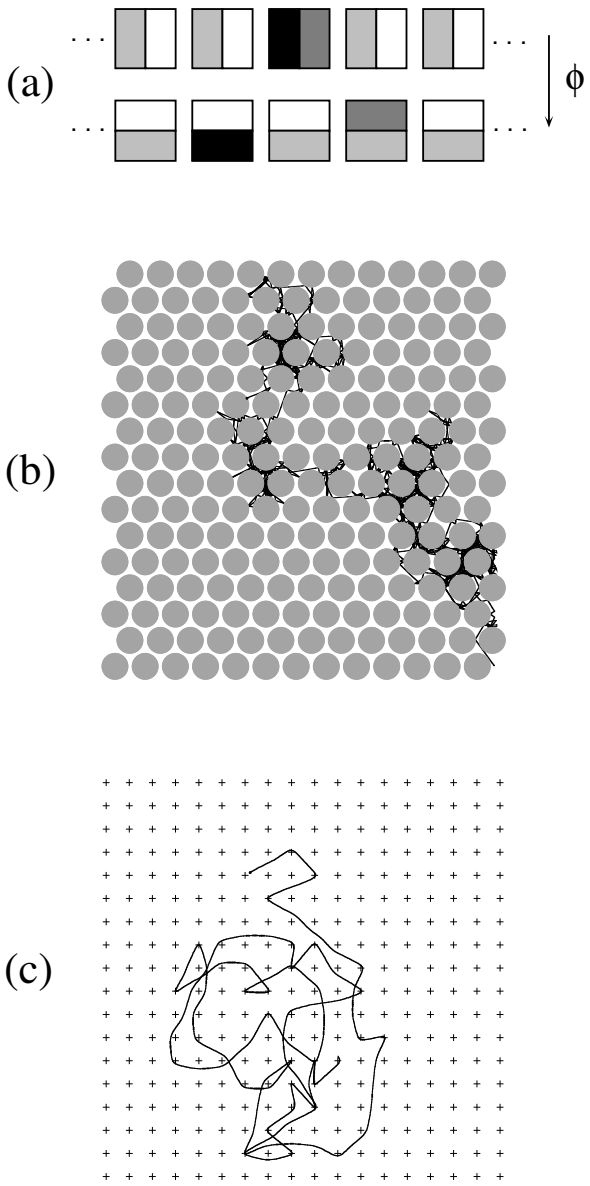

FIG. 1: (a) Dyadic multibaker map ϕ acting on a chain of squares. (b) Trajectory of a particle of unit velocity in the hard-disk Lorentz gas of interdisk distance $d = 2.3$; (c) Trajectory of a particle of mass $m = 1$ and energy $E = 3$ in the Yukawa-potential Lorentz gas of inverse screening length $\alpha = 2$.

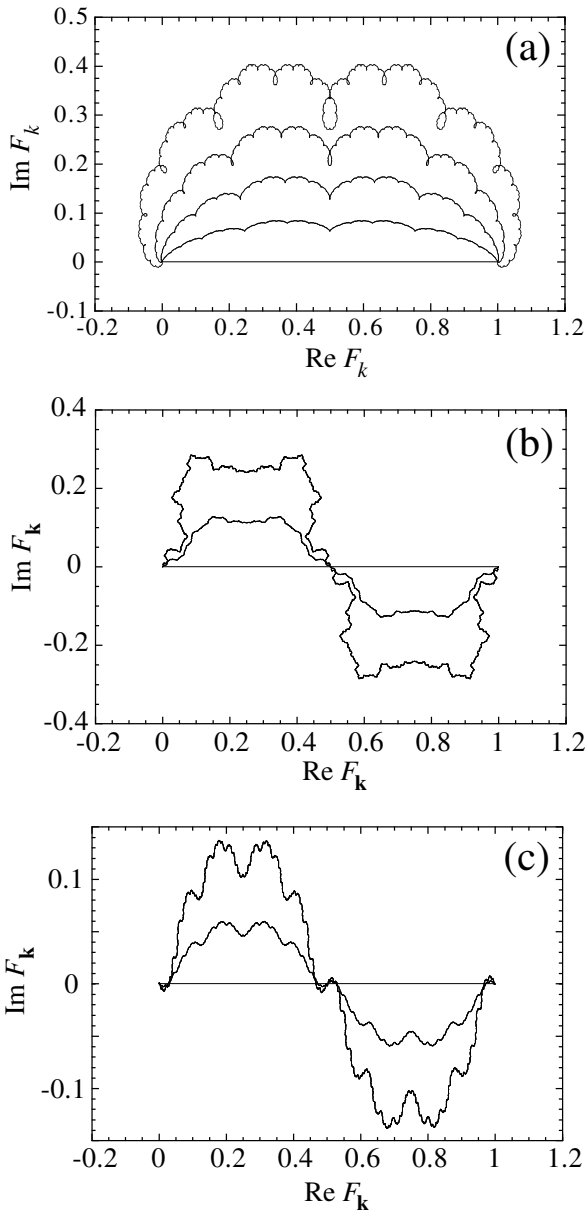

FIG. 2: Cumulative functions (8) of the hydrodynamic modes of diffusion: (a) of wavenumber $k = 0.0$, 0.25, 0.5, 0.75, 1.0 for the dyadic multibaker map; (b) of wavenumbers $k_x = 0.0$, 0.5, 0.9 and $k_y = 0$ for the hard-disk Lorentz gas of interdisk distance $d = 2.3$ and unit velocity; (c) of wavenumbers $k_x = 0.0$, 0.2, 0.4 and $k_y = 0$ for the Yukawa-potential Lorentz gas of mass $m = 1$, energy $E = 3$, and inverse screening length $\alpha = 2$.

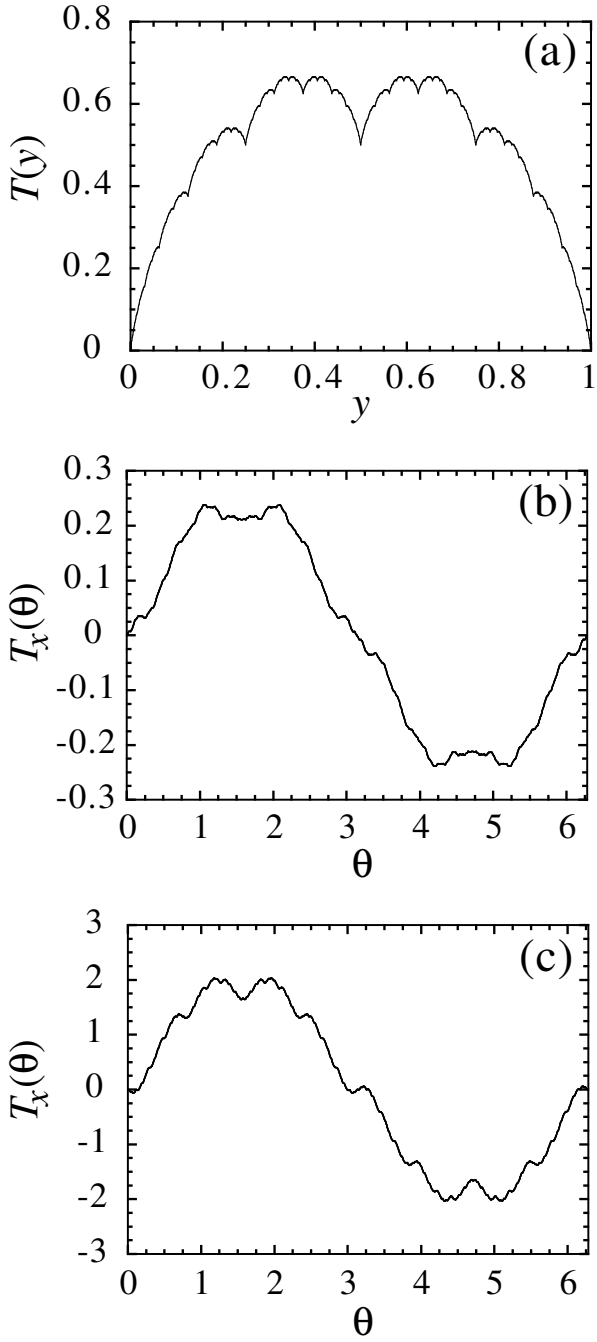

FIG. 3: Cumulative functions (12) of the nonequilibrium steady state of diffusion: (a) for the dyadic multibaker map; (b) of gradient in the x-direction for the hard-disk Lorentz gas of interdisk distance $d = 2.3$ and unit velocity; (c) of gradient in the x-direction for the Yukawa-potential Lorentz gas of mass $m = 1$, energy $E = 3$, and inverse screening length $\alpha = 2$.

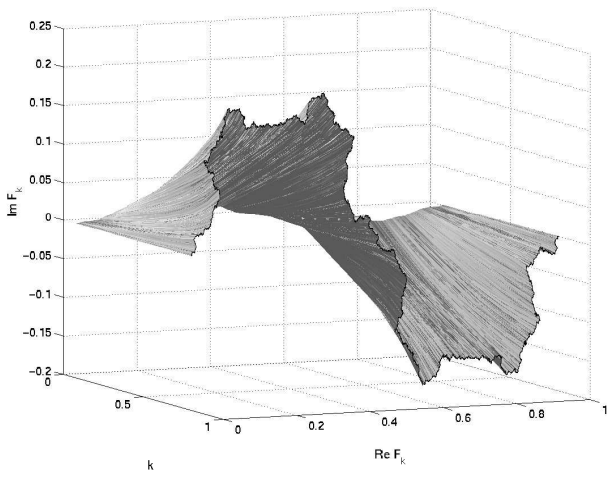

FIG. 4: Three-dimensional representation of the cumulative functions of the reactive modes of relaxation in the 2D reactive periodic Lorentz gas of interdisk distance $d = 2.3$, reaction probability $p_0 = 0.3$, and one catalyst per $N = 3$ disks. $(\mathrm{Re}F_k, \mathrm{Im}F_k)$ is depicted in the complex plane as a function of the wavenumber k.